1973

A visualization study of secondary flows in planar nozzles

Ahmed N. Siddiqui
Lehigh University

A VISUALIZATION STUDY OF SECONDARY FLOWS IN PLANAR NOZZLES

by

Ahmed Nadim Siddiqui

A Thesis
Presented to the Graduate Committee
of Lehigh University
in Candidacy for the Degree of
Master of Science
in
The Department of Mechanical Engineering and Mechanics

Lehigh University
1972

This thesis is accepted and approved in partial fulfillment of the requirements for the degree of Master of Science.

November 22, 1972
(date)

Jerry A. Bowers
Professor in Charge

Richard P. Dodge
Chairman of Department

ACKNOWLEDGEMENT

Throughout this study, the author received most valuable guidance and constant assistance in experiments from his teacher and thesis adviser, Dr. Jerzy A. Owczarek, to whom the author wishes to express his gratitude.

The work was supported by the Office of Naval Research under Contract No. N00014-69-A-0417.

TABLE OF CONTENTS

ABSTRACT

The purpose behind the experimentation was to obtain a better understanding of the secondary flows associated with the flows from convergent planar nozzles preceded by a circular duct.

The flow visualization was achieved by injecting smoke upstream of the rectangular nozzle inlet. The tests were carried out using different nozzles with some geometrical variations. The effect of Reynolds number on the flow pattern for each of these nozzles was also studied. The tests were run at low Mach numbers. Photographs of the flow pattern were taken at nozzle exits by illuminating only that plane.

A distinct configuration of vortices in the exit passage was observed which was in general common for every nozzle geometry. In addition, each nozzle geometry produced its own pattern which was distinct from the others. The axes of the vortices observed have the general direction of the main flow.

It was observed that the flow was not very sensitive to the upstream conditions, for example, to the location of the flow straightener (if it was not placed very close to the nozzle inlet), and of the screens in the stagnation tank.

Smoke injection was carried out so as to produce minimal flow disturbance in the stagnation tank.

1. INTRODUCTION

The performance of fluid amplifiers depends, among other things, on the uniformity of the flow leaving the supply nozzle. The performance of the amplifier can be expected to become increasingly inconsistent with increasing nonuniformity of the flow. The object of this study was to investigate the characteristics of the flow patterns in planar nozzles (having low exit passage aspect ratios) by the method of smoke visualization. The planar nozzles used in the experiments were of the type commonly used in fluid amplifiers.

An extensive study of secondary flows in turbine nozzle cascades has been made earlier by Herzig, Hansen and Costello [1], by Rohlik, Kofskey, Allen and Herzig [2] and by Senoo [3]*.

Herzig, Hansen and Costello conducted a smoke visualization study of secondary flows in cascades of turbomachinery. Their photographs show the migration of the end wall boundary layer towards the suction surface at the turning of the mainstream in the cascade, which was followed by a three-dimensional roll-up of the end wall boundary layer in a region near the suction surface to form a passage vortex. The size and tightness of this passage vortex was found to depend

*Numbers in brackets refer to references at the end of the text.

mainly upon the turning of the mainstream. Their conclusion was that the passage vortex formation is the principal secondary flow phenomenon in rectangular bends, as it is in cascades. However, the boundary layer flows in cascades are noticeably different from those in bends.

Rohlik, Kofskey, Allen and Herzig observed in their experiments two secondary flow patterns: a cross-passage boundary layer flow on the end wall from the pressure surfaces to the suction surfaces, and a radial flow inwards along the trailing edges of the blades. They also found that the magnitude and extent of the blade wakes is dependent upon secondary flow conditions.

Senoo conducted his experiments with turbine nozzle cascades by taking pressure measurements along the end wall of the cascade. His investigations revealed that the part of secondary flow in the nozzle, which is related to the upstream boundary layer, depends upon the configuration of the nozzle. His measurements also showed the end wall boundary layer rolling up at the suction surface end wall corner of the cascade. The cross flow in the end wall boundary layer was explained by the pressure gradient effects induced in the boundary layer flow by the inviscid main flow. Norbury [4] made experimental investigations of flows through a two-dimensional diffuser. Measurements were made of the growth

of the boundary layers on both the divergent and parallel walls and visual flow experiments were carried out. In his experiments he found the presence of vortices localized in the corners of the duct.

Moore and Kline [5] in their study of two-dimensional subsonic diffusers used water having a free surface. They observed secondary flows occupying the whole cross-section of the diffuser at the throat. These secondary flows were attributed to the curvature of the streamlines near the cylindrical wall at the edge of the diffuser throat.

Stanitz, Osborn and Mizisin [6] conducted experiments to investigate secondary flows in a rectangular elbow with 90° of turning. Boundary layer separation was prevented by avoiding local deceleration along the walls. Secondary flows were investigated for six boundary layer thicknesses. From their experiments they concluded that the passage vortex associated with the secondary flows in elbows might be considered to be formed by folding up of constant total pressure surfaces (Bernoulli surfaces) and then, the eventual winding up of the streamlines, which lie on these surfaces, into a tight spiral. The passage vortex appeared to be near the suction surface and away from the plane wall of the elbow. As the boundary layer size increased a sudden difference in secondary flow occurred, perhaps associated with the reduced importance of viscous effects in the thick boundary layer. Also it was concluded that the strength of the secondary

vortices is small and the energy of the secondary flow is small.

Experimental studies of flows in planar nozzles were made at Lehigh University by Owczarek, Rockwell, Cha and Wagner [7, 8, 9].

In experiments reported in references 7 and 8, total pressure traverses were made along the exit plane of the nozzles to determine the total pressure losses associated with these secondary flows. These traverses revealed the existence of concentrated regions of large total pressure losses near the upper and lower walls of the nozzles extending, in general, well into the main flow. Different nozzles with geometrical variations were used. Along the horizontal walls of the nozzle exit (upper and lower walls), four regions of low total pressure were observed. Two of them were located near the side walls, and two near the midplane of the exit passage. Thus four corner loss regions and four midplane loss regions were observed in these nozzles. These loss regions were partly submerged in the boundary layer flow and partly extended into the main flow. The largest magnitude of the total pressure loss measured in these regions outside of the normal boundary layer flow was of the order of 70 percent of the available dynamic pressure.

With the absence of a convex wall contour in the planar nozzle, only the four regions of low total pressure in the

vicinity of the midplane were observed. They were of small magnitude and were buried well within the thin boundary layer flow. The corner loss regions were absent.

The corner loss regions were attributed to the secondary flows resulting from the boundary layer migration of the side wall boundary layer. This secondary flow resulted from the radial pressure gradient of the main flow produced by the convex nozzle wall contour, and imposed on the boundary layer flow. Flow visualization tests using smoke and thread probes showed that single vortical motion was present in each corner total pressure loss region. The secondary flows caused by the rectangular inlet to the nozzle were found to be responsible for midplane pressure losses.

Wagner, in his experiments using nozzles having smaller aspect ratio of the rectangular inlet than that used in the tests reported above, observed, in addition to the corner loss regions in general four pressure loss regions on each side of the midplane. The occurrence of the total pressure loss regions on each side of the midplane on the top and bottom nozzle exit walls was not very consistent.

2. DESCRIPTION OF APPARATUS

2.1 Test Rigs and Smoke Injector

The experiments were carried out on two test rigs used in the studies reported in references 7, 8, and 9. They are shown in Figures 1 and 2.

Figure 1 shows test rig with an 8 inch I.D. stagnation tank. Starting from the air inlet in the downstream direction, the stagnation tank incorporated two adjacent fine mesh screens followed by a flow straightener (3 1/2" long with 1/8" hexagonal cells). Further down two "crescent-shaped" smoke injectors were provided, each made up of 5" long copper tubing (approximately 0.25" I.D.) with 10 outlet holes each pointing downstream. An 1/8" diameter brass tube supported the injectors in the stagnation tank through which smoke was introduced. By moving these brass tubes in and out the position of these smoke injectors inside the stagnation tank could be adjusted. Following these was another fine mesh screen which was provided there to smooth out any disturbances created by these smoke injectors. These screens block 70 percent of the flow area of the tanks and hence help to distribute the flow evenly in the whole cross-section of the stagnation tank. Further down the screen and about an inch away from the rectangular nozzle inlet was a circular smoke injector circumscribing the inner periphery of the

stagnation tank. This injector was also made out of 0.25" I.D. copper tubing with 8 inlet holes and 42 outlet holes for smoke. The reason for having so many outlet holes was twofold. First, to obtain a curtain of smoke around the circumference and secondly, to restrict the velocity of smoke entering the stagnation tank to a minimum, so as to have minimal disturbance of the flow. To avoid separation of flow near the walls adjacent to this circular injector, a smooth transition of flow over the injector was provided as shown in Figure 1. The rectangular inlet to the nozzle had rounded leading edges to channel the flow from the stagnation tank to the nozzle.

Two convergent nozzles were used separately for experiments with this set-up. Both nozzles were of the concave-convex type with certain geometrical variations as shown in Figure 3. Nozzle A had an exit passage aspect ratio of 5 and nozzle M, an exit passage aspect ratio of 4. The area contraction ratio of nozzle A was 11.25 and that of nozzle M was 9.

The whole test rig was set up vertically to ensure an even distribution of smoke. It was observed that the smoke drifted downwards under the action of gravity when the test rig was set horizontally, which deprived the upper section of the nozzle of smoke.

Dry and clean air to the top of the stagnation tank was supplied through a flowmeter and control valves from a large reservoir where constant pressure was maintained.

Figure 2 shows the second test rig, having 6" I.D. stagnation tank. Downstream of the air inlet was incorporated a fine mesh screen followed by a honeycomb flow straightener (3 1/2" long with 1/8" hexagonal cells). Downstream of the flow straightener were two crescent-shaped smoke injectors (described above) followed by two screens. Immediately following these screens was a circular smoke injector. This circular smoke injector was also made of copper tubing. It had 3 inlet and 50 outlet holes for the passage of smoke from the smoke generator into the stagnation tank. Following the circular injector was a fine screen. A 6" I.D. stagnation tank section 12" long followed, which led to the rectangular nozzle inlet. The edges of the inlet were rounded off to facilitate the smooth transition of flow from the circular to the rectangular duct.

For the tests, two types of convergent nozzles were used with this test rig. Figure 4 shows the geometries of nozzles A_{sm} and B_{sm}. Nozzle A_{sm} was the concave-convex type. In nozzle B_{sm}, the concave part was followed by a straight section. The exit passage aspect ratio of both of these nozzles was 3, with the area contraction ratio of 17.

The test rig was set up vertically for reasons explained above.

2.2 Smoke Generator

Figure 5 explains the simple method used for the generation of smoke for the experiments. A lighted cigar was inserted into one section of the tube, which fitted into one end of another tube of larger diameter by means of a rubber cork. Through the other end of the larger diameter tube dry and clean air was introduced which after passing through the cigar carried the smoke to the smoke injectors via a small network of plastic tubing.

2.3 Photographic Equipment and Arrangement

A Nikon-F camera with a telephoto lens (1:3.5, f = 13.5 cms.) was used along with the Nikon Bellows focusing attachment. This attachment made possible the close-up focusing of the whole nozzle exit in the view finder from a distance of about 16".

The two walls of the planar nozzle were covered with black paper from the outside with slits cut in the paper on each side at the nozzle exit. They were approximately 1/16" wide and extended over the nozzle exit. Light was focused at these slits by means of two Kodak slide projectors (600 watt lamps each) placed on each side of the wall. The rest of the test rig was covered with paper to avoid any entrance of light. In this way only the exit plane of the nozzle was illuminated.

3. TEST RESULTS

3.1 Pressure Measurements on Face of Nozzle Inlet Plate

In order to determine the pressure distribution on the face of the flat surface having the rounded rectangular nozzle inlet, pressure taps were provided at various locations on that face. The purpose of this test was to learn about the origin of the secondary flows in the midplane of the nozzle. A total pressure tap on top of the stagnation tank was also provided. These pressure taps were connected to a water manometer. To begin with, the experiments were run at low Reynolds numbers on a 6" stagnation tank rig with 5 pressure taps on the nozzle inlet flange. Very small pressure differences were observed between these taps (approximately 0.02" to 0.03" of water). No conclusions could be drawn from these tests. Reason for the small pressure differences could be explained by the fact that the difference between total pressure in the stagnation tank and the atmospheric pressure was of the order of 0.1" of water. Since the total pressure in the tank is small, very slight differences in pressures between the taps should exist.

To verify the existence of pressure gradient, large velocity at exit from the tank was needed, since

$$\frac{\partial P}{\partial R} = -\rho \frac{V^2}{R}$$

that is,

$$\frac{\partial P}{\partial R} \propto V^2$$

Therefore, in order to increase the total pressure and flow velocity in the stagnation tank it was decided to decrease the diameter of the stagnation tank from 6" to 3.5", and to run the experiments at higher Reynolds numbers. Also, the number of pressure taps on the plates was increased, with one plate having as many as 32 pressure taps in one quadrant of its circular section. Two rectangular and one square nozzle inlets were tried having the same areas (see Figure 6). Tests were run first with sharp inlet edges and later with the edges rounded off. The only difference between the two tests was that at the same flow rate, the total pressure reading in the stagnation tank was higher in the sharp edged inlet than when it was rounded off. This can be explained by the fact of the vena contracta formation in the sharp edge case.

The pressure difference between the various pressure taps was still found to be too small to allow definite conclusions to be drawn.

3.2 Development of Smoke Visualization Technique

The injection of smoke in the stagnation tank for the purpose of visualization of secondary flows at the nozzle exit posed a few problems. The idea was to distribute the smoke evenly around the periphery of the circular section of the stagnation tank with minimum disturbance to the flow, so that when smoke entered the nozzle it would circumscribe the nozzle perimeter. The location and arrangement of the smoke injectors was observed to have an influence on the stability of the pattern of vortices at the exit passage of the nozzle.

To begin with, the experimental rig was kept horizontal. Smoke was injected from about 12" upstream of the nozzle inlet by means of three streamlined "bullet-shaped" smoke injectors located at 120° intervals around the circumference, with the smoke directed downstream towards the nozzle inlet. It was observed that the smoke from the injector located at the top of the stagnation tank drifted downwards under the action of gravity and did not follow the stagnation tank walls as was desired. This way, the top section of the nozzle was deprived of smoke with excess smoke in the lower section. To avoid this problem, four smoke injectors, located just next to the nozzle inlet (possibly in the separated region) were tried. This way the smoke distribution in the nozzle improved considerably, but it was observed that by injecting the smoke so close to the nozzle inlet disturbed the flow and the vortices in the exit passage were very unsteady.

Injection of smoke was also tried at the very inlet to the test rig by placing the smoke injector in the air inlet pipe. This way the smoke got diffused throughout the whole section and it was not possible to observe clearly the vortices.

It was noted that by placing the smoke injectors upstream of the flow straightener, a pattern of small honeycomb cells was present in the nozzle exit passage along with the regular pattern of vortices. This cell pattern was obviously due to the wakes formed by the honeycomb flow straightener and was not in any way associated with the flow pattern in the nozzle. Thereafter, the flow straightener was placed upstream of the smoke injectors.

To eliminate the problem of smoke drifting downwards under the action of gravity, the whole experimental rig was set up vertically so that the flow was now from top to bottom instead of in a horizontal direction. To get a better distribution of smoke, eight smoke injectors were provided at equal intervals around the circumference about 9 inches upstream of the nozzle inlet. A fine screen was placed just downstream of the injectors to smooth out any turbulence inflow caused by the injectors, and also to diffuse the smoke to some extent. The smoke distribution was uniform around the periphery with this arrangement, but it was observed now that the smoke, after settling down around the nozzle inlet, preferred to follow certain specific paths. The two parallel

walls of the planar nozzle were deprived of the smoke in this way. The reason for this was that along the flat face of the nozzle inlet plate, there were regions of high pressure around the two parallel walls. The smoke therefore was forced to move in the nozzle passage, away from these high pressure regions, from the top and bottom wall (see Figure 7), avoiding the side walls. Another set of smoke injectors was needed therefore, which could supply smoke to these two walls.

The arrangement which was finally adopted and was found suitable was a circular smoke injector described earlier (Figure 1), which distributed smoke along the top and bottom walls of the nozzle and also to the corners, and two crescent-shaped smoke injectors upstream, which protruded inside the stagnation tank and supplied smoke to the two side walls of the nozzle. The position of these crescent-shaped injectors inside the stagnation tank could be adjusted.

Regulation of the quantity of smoke through the smoke injectors was another factor of importance. Too little smoke did not cover the whole flow field, and on the other hand, too much smoke caused the vortices to distort or become abnormally large. To avoid this, the amount of smoke flow was constantly regulated.

During the tests, tar from the cigar smoke was slowly condensing in the plastic tubes supplying the smoke to the

injectors. When the amount of tar acumulated became large, the supply of smoke through the injectors became erratic, the influence of which could be detected in the flow pattern. It was therefore necessary to drain the tar from the tubes every now and then.

3.3 Tests with Nozzle A

The tests with nozzle A were run at four different values of Reynolds number. The Reynolds number was based on the nozzle width of 0.48" (characteristic length), and on the mean exit flow speed.

Figure 8 shows the pattern of vortices at the exit passage of nozzle A at $Re_w = 3.9 \times 10^3$. The exit passage aspect ratio for nozzle A was 5.

Four vortices, two on each side of the midplane, can be seen on the top and bottom wall of the nozzle. These top and bottom wall vortices were always present in the form of "mushroom" like pairs with a "stem" attaching them to the walls. The direction of the vortices appearing in pairs is opposite to one another. These vortices are asymmetric about the midplane and their position along the top and bottom wall varies. Figure 8(a) shows the bottom wall pairs of vortices being further apart than the same pairs in Figure 8(b). The origin of the above vortices can be traced back

to the nozzle inlet. Regions of high pressure along the parallel walls of the nozzle inlet on the flat face compelled the flow to go around it and enter the nozzle passage from the top and bottom walls. The interaction of this cross-flow with the main flow at the nozzle inlet leads to the formation of the top and bottom wall vortices. Figure 7(c) explains the flow pattern along the flat face of the nozzle inlet plate. In each corner of the nozzle exit passage a vortex is present. These corner vortices had their direction of roll-up away from the side walls. The origin of these vortices is attributed to the boundary layer migration along the parallel walls, away from the centerplane. The pressure gradients imposed on the boundary layer by the main flow because of the convex wall contour of the nozzle, are responsible for this migration. Figure 8(a) and 8(b) show very clearly the origin of these corner vortices from somewhere close to the centerplane. Due to the cross-flow in the boundary layer, fluid travels along the side walls on each side of the centerplane and away from it towards the top and bottom wall where it rolls up into a vortex. Each of these corner vortices seems to give rise to another vortex in the opposite direction near the centerplane of the nozzle and close to the side walls.

The centerplane vortices, though not clearly defined in Figure 8, are definitely present. The boundary layer migration along the planar wall (because of the concave wall

contour of the nozzle) is responsible for these centerplane vortices. Here, the cross-flow in the boundary layer is towards the centerplane from both sides. The interaction of the cross-flow is at the centerplane resulting in two vortices in opposite directions stemming out of the side wall.

The boundary layer migration along the parallel walls is shown in Figure 7(a).

Figure 9 shows the exit passage pattern at Reynolds number 5.3×10^3. The pattern is essentially the same as before. Figure 9(a) shows the centerplane vortices very clearly. It will be noticed that the right hand side centerplane vortices in Figure 9(a) have another pair of vortices stemming out of the lower vortex. Later photographs show as many as 3 pairs of vortices associated with the centerplane. The occurrence of more than one pair of vortices at the centerplane is difficult to explain. Figure 9(b) shows the result of too much smoke along the right wall. The right hand side centerplane vortices have extended deep into the nozzle. Distortion of the mushroom-shaped vortices on the lower wall is evident as the centerplane vortices push on it.

Figure 10(a) shows exit passage pattern at Reynolds number 6.87×10^3. Four corner vortices and the centerplane pairs of vortices can be clearly seen. The top and bottom wall vortices become increasingly unsteady and turbulent with

increased Reynolds number with their position along the top and bottom wall constantly fluctuating. Two pairs of vortices on the top wall are evident while on the bottom wall the two pairs appear to be colliding with each other with the left pair extending all the way near to the left wall.

Figure 10(b) shows the flow pattern at Reynolds number 7.4×10^3. Only one corner vortex in the lower left hand corner can be seen. This is only due to the lack of smoke in the other corners. Two pairs of centerplane vortices near each side wall can be seen. All the four top and bottom wall pairs are present here. They appear to be hazy and blurred because of the increasing turbulence in the flow.

It should be noted that as the Reynolds number increases the vortices become "tighter".

3.4 Tests with Nozzle M

The difference between geometry of nozzle M and Nozzle A can be seen in Figure 3. Tests with nozzle M were run at 3 different Reynolds numbers, based on the width of the nozzle (0.6 inches) and the mean exit flow speed.

Figure 11(a) and 11(b) show the flow pattern at the exit passage at $Re_W = 3.9 \times 10^3$. The pattern observed here is essentially the same as in nozzle A and as one would expect in a concave-convex nozzle. It is however interesting to note

that the centerplane vortices extend deeper into the exit passage of the nozzle. This may be due to the extended straight section between the concave and convex wall contour of the nozzle. The two pairs of vortices on the top and bottom wall in Figure 11(b) are further apart than the same vortices in Figure 11(a).

Figures 12(a) and 12(b) show the flow patterns at exit at $Re_w = 5.3 \times 10^3$. Figure 12(a) shows very clearly the patterns explained earlier. Figure 12(b) shows the right hand side centerplane vortices extending towards the upper wall. This abnormal behavior might be due to some upstream disturbances in the flow.

Figures 13(a) and 13(b) show the effects of excessive smoke in the test section. The Reynolds number is the same as for in Figure 12 ($Re_w = 5.3 \times 10^3$). It is interesting to note in Figure 13(a) that the centerplane vortices extend all the way to the midplane, flattening out the top and bottom vortices. In Figure 13(b) the two pairs of centerplane vortices have crossed each other and are locked in that position. It was seen that when the quantity of smoke was gradually decreased, these centerplane vortices tended to stay locked in that position even for normal flow of smoke. Figure 13(b) shows the top wall pairs and one of the bottom wall pair to be flattened out by this disturbance. In addition, two more pairs of vortices on the right hand side wall can be

seen stemming out from near the vicinity of the centerplane.

Figures 14(a) and 14(b) show the flow pattern at Re_w = 7.4×10^3. As can be observed the top and bottom wall pairs of vortices are unsteady and turbulent at this higher Reynolds number. The same was observed in experiments with nozzle A. Figure 14(a) seems to show 3 pairs of vortices on the top and bottom wall at this Reynolds number.

3.5 Tests with Nozzle A_{sm}

The geometry of nozzle A_{sm} is similar to that of nozzle A (Figure 4). The inlet aspect ratio of nozzle A_{sm} was 5.67 which is higher than that of the inlet aspect ratio of nozzle A. The exit aspect ratio is 3.

Figures 15(a) and 15(b) show the flow patterns at the exit passage of nozzle A_{sm} at Reynolds number = 6.7×10^3. Four corner vortices and two pairs of centerplane vortices can be seen. The corner vortices, as is evident from Figures 15(a) and 15(b), pick up fluid from the top and bottom wall boundary layer. The top and bottom wall vortices are not very well formed at this low Reynolds number. This may be explained by the fact that at this Reynolds number, the secondary flow at the inlet to the nozzle does not have sufficient momentum which is required for these vortices to form.

Figures 16(a) and 16(b) show the flow pattern at Re_w = 8.5×10^3. In addition to the corner and centerplane

vortices, we have one pair of midplane vortices each, on the top and bottom wall. In Figure 16(b) the midplane pair of vortices on the upper wall is seen in the process of developing into a healthy pair as in Figure 16(a).

Figures 17(a) and 17(b) show the flow pattern at Re_W = 1.26×10^4. In Figure 17(a) four corner vortices and two pairs of centerplane vortices can be seen. On the top wall, one midplane pair of vortices is present while on the bottom wall two pairs of vortices are evident. From this it can be inferred that the top and bottom wall vortices can occur either in single or in double pairs in this nozzle. In Figure 17(b) the midplane vortices occur in single pairs on both upper and lower walls. The origin of these midplane vortices is explained in Figure 7(b).

To have an idea of how this pattern of vortices changes downstream of the exit passage, photographs were taken in a plane 0.5" downstream of the exit passage. Figure 18(a) shows the corner and centerplane vortices still quite evident in the flow, while the top and bottom vortices are seen to diffuse rapidly in the flow downstream of the exit passage.

3.6 Tests with Nozzle B_{sm}

The geometry of nozzle B_{sm} is shown in Figure 4. Figure 18(b) shows the pattern at $Re_W = 8.5 \times 10^3$. Existence of the midplane vortices on the top and bottom wall, and the

centerplane vortices can be made out, though it is not very clear. Unfortunately, better photographs of the flow pattern in this nozzle could not be obtained.

The absence of corner vortices in nozzle B_{sm} can be explained by the fact that the convex wall contour, which is responsible for their generation, was absent in this nozzle.

4. CONCLUSIONS

This experimental investigation has shown that:

1. The geometry of the planar convergent nozzles has a marked influence on the degree of nonuniformity of flow at the exit passage.

2. Planar convergent nozzles having concave-convex inner walls and rectangular rounded inlets, produce nonuniform flow at the exit near the upper and lower walls in the vicinity of the side walls, and near the side walls at the centerplane. These regions of nonuniform flow are caused by a secondary flow produced by migration and roll-up of side wall boundary layer in the vicinity of the concave and convex wall contours. The migration of the side wall boundary layer is caused by the pressure gradient of the main flow. This nonuniform flow, present in the form of concentrated vortices, has under its influence a considerable area of the exit cross section. The axes of these vortices have the general direction of the main flow.

3. Planar nozzles having concave-convex inner walls and rectangular inlets with circular ducts upstream, can produce nonuniform total pressure distribution in the flow at the exit near the upper and lower walls in the vicinity of the midplane. These midplane regions of nonuniform flow are generated by a spiral flow caused by the rectangular inlet

to the nozzle. This secondary flow was found to be sensitive to the Reynolds number, becoming increasingly unsteady with increasing Reynolds number.

The inlet aspect ratio of the rectangular inlet has a large effect on the top and bottom wall pairs of vortices. They tend to occur in single pairs in the midplane for a high value of inlet aspect ratio, while for a lower value they occur in double pairs, and on each side of the midplane.

4. Planar convergent nozzles having a concave-straight inner wall profile and rectangular inlets with circular ducts upstream can produce secondary flows (vortices) in the centerplane due to the concave wall contour and on the top and bottom walls in the vicinity of the midplane due to the rectangular inlet. The vortices on the top and bottom wall observed in this nozzle did not extend very deep into the main flow.

5. REFERENCES

1. Herzig, H.Z., Hansen, A.G., and Costello, G.R., "A visualization Study of Secondary Flows in Cascades", NACA Report 1163, 1953.

2. Rohlik, H.E., Kofskey, M.G., Allen, H.W., and Herzig, H. Z., "Secondary Flows and Boundary Layer Accumulation in Turbine Nozzles", NACA Report 1168, 1953.

3. Senoo, Y., "The Boundary Layer on the End Wall of a Turbine Nozzle Cascade", Trans. ASME, Vol. 80, 1958, pp. 1171-1720.

4. Norbury, J.F., "Some Measurements of Boundary Growth in a Two-Dimensional Diffuser", Journal of Basic Engineering Trans. ASME, Series D, Vol. 81, No. 3, Sept. 1959, pp. 285-296.

5. Moore, C.A., Jr. and Kline, S.J., "Some Effects of Vanes and of Turbulence in Two-Dimensional Wide-Angle Subsonic Diffusers", NACA TN 4080, June 1958.

6. Stanitz, J.D., Osborn, W.M., and Mizisin, J., "An Experimental Investigation of Secondary Flow in an Accelerating, Rectangular Elbow with 90° of Turning", NACA TN 3015, October 1953.

7. Owczarek, J.A., Rockwell, D.O., and Cha, Y.S., "A Study of Flow From Two Planar Nozzles", Lehigh University, Project Fluid Amplifiers Technical Report No. 1, June 1970.

8. Owczarek, J.A. and Rockwell, D.O., "An Experimental Study of Flows in Planar Nozzles", Trans. ASME, Vol. 94, Series D, No. 3, September 1972, pp. 682-688.

9. Wagner, W.B. and Owczarek, J.A., "A Study of Flow Fields in Bistable Fluid Amplifiers - Part I: Experimental Investigation", Lehigh University, Project Fluid Amplifiers Technical Report No. 9, June 1972.

VITA

Ahmed Nadim Siddiqui was born in Rawalpindi (Pakistan) on March 1, 1949. He is the son of Farhat and Moinriddin Siddiqui.

He had his elementary and college education in Karachi. He graduated from N. E. D. Government Engineering College, Karachi, with a Bachelor's Degree in Mechanical Engineering in September 1970.

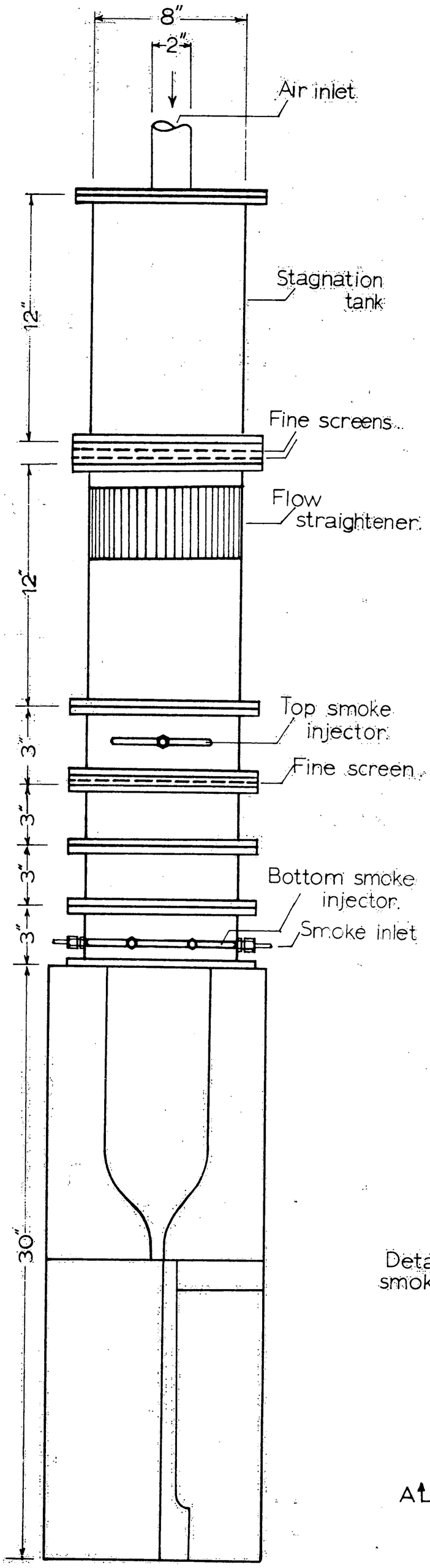

Detail of experimental rig

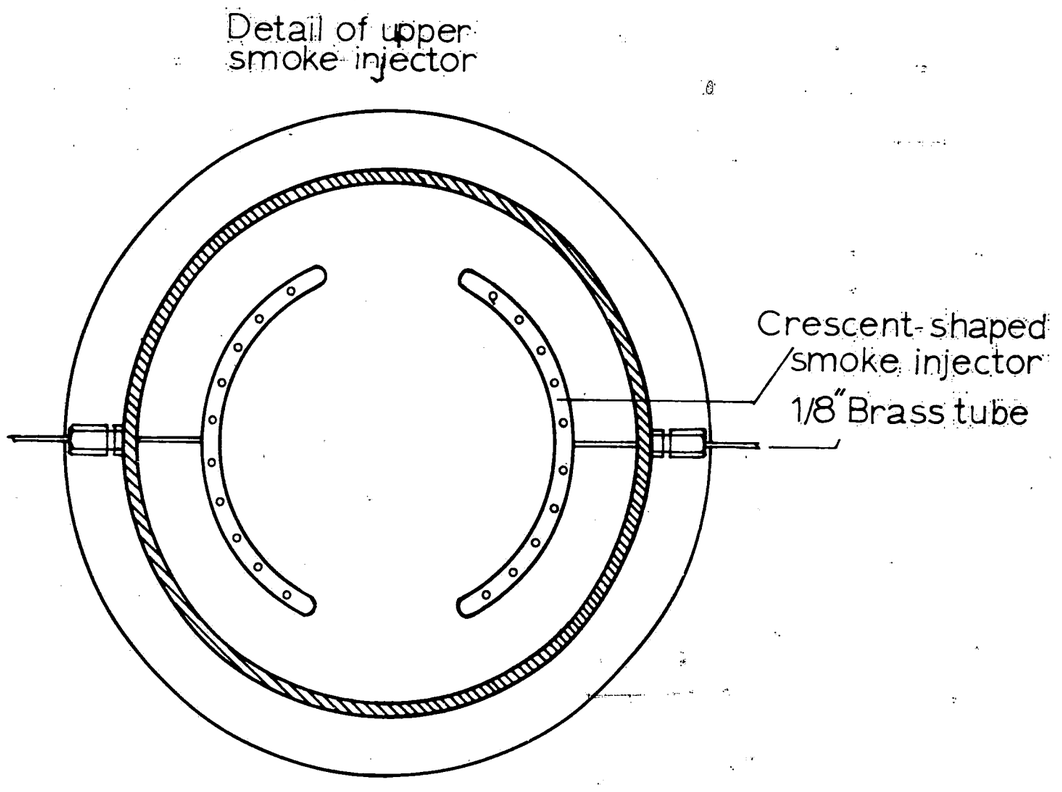

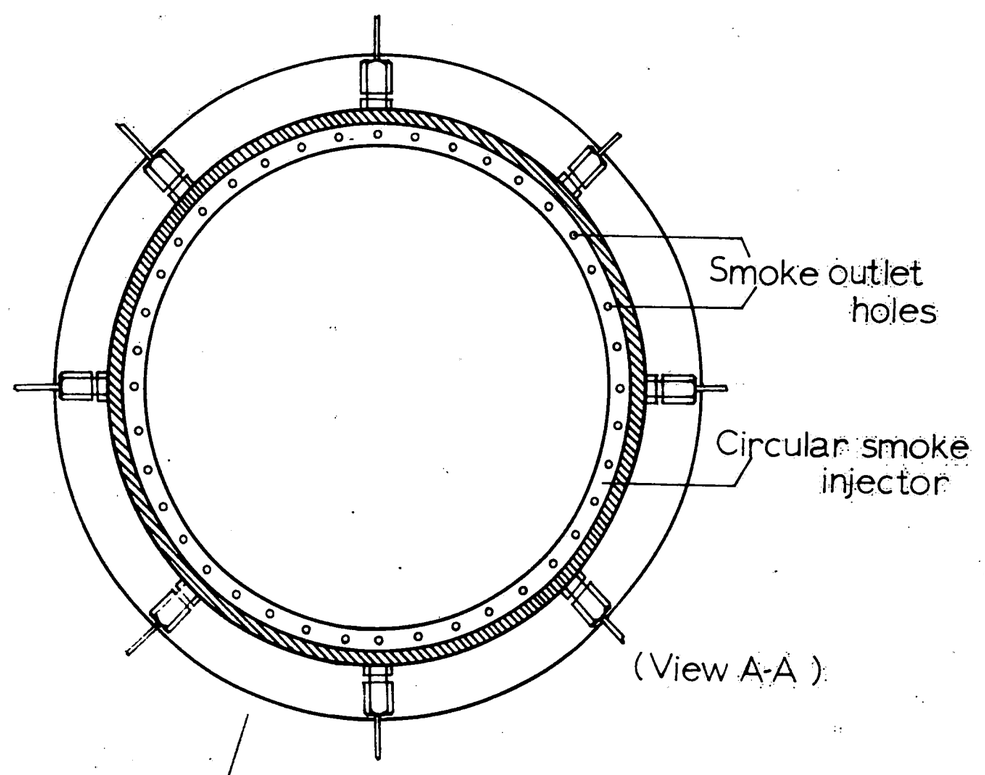

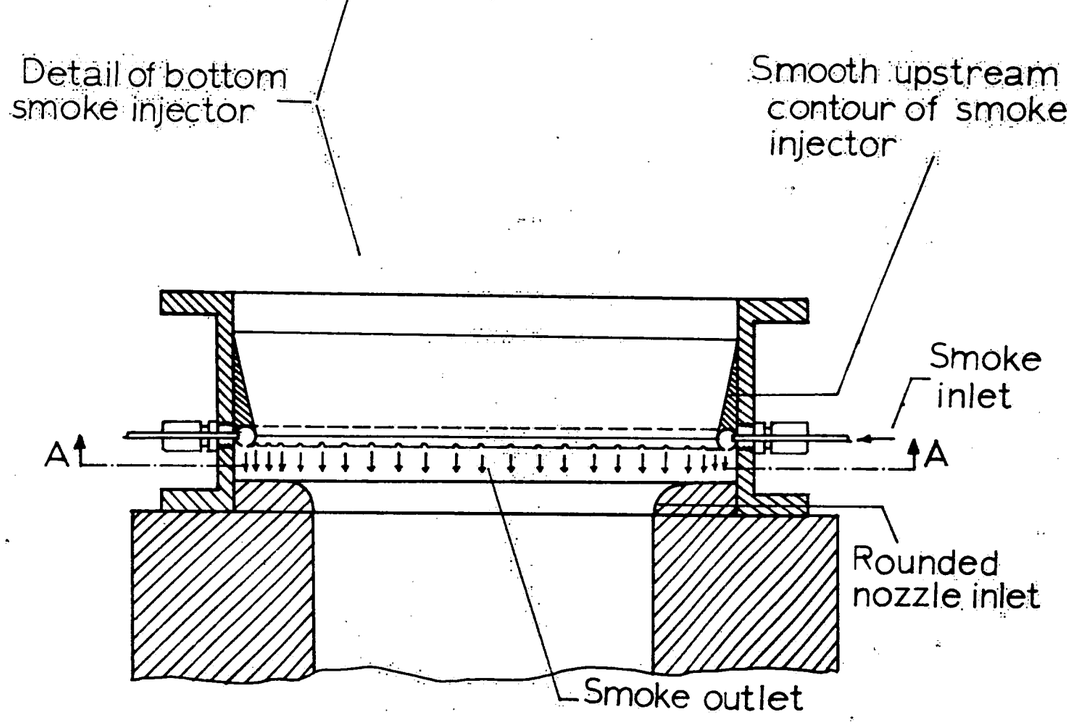

FIGURE 1

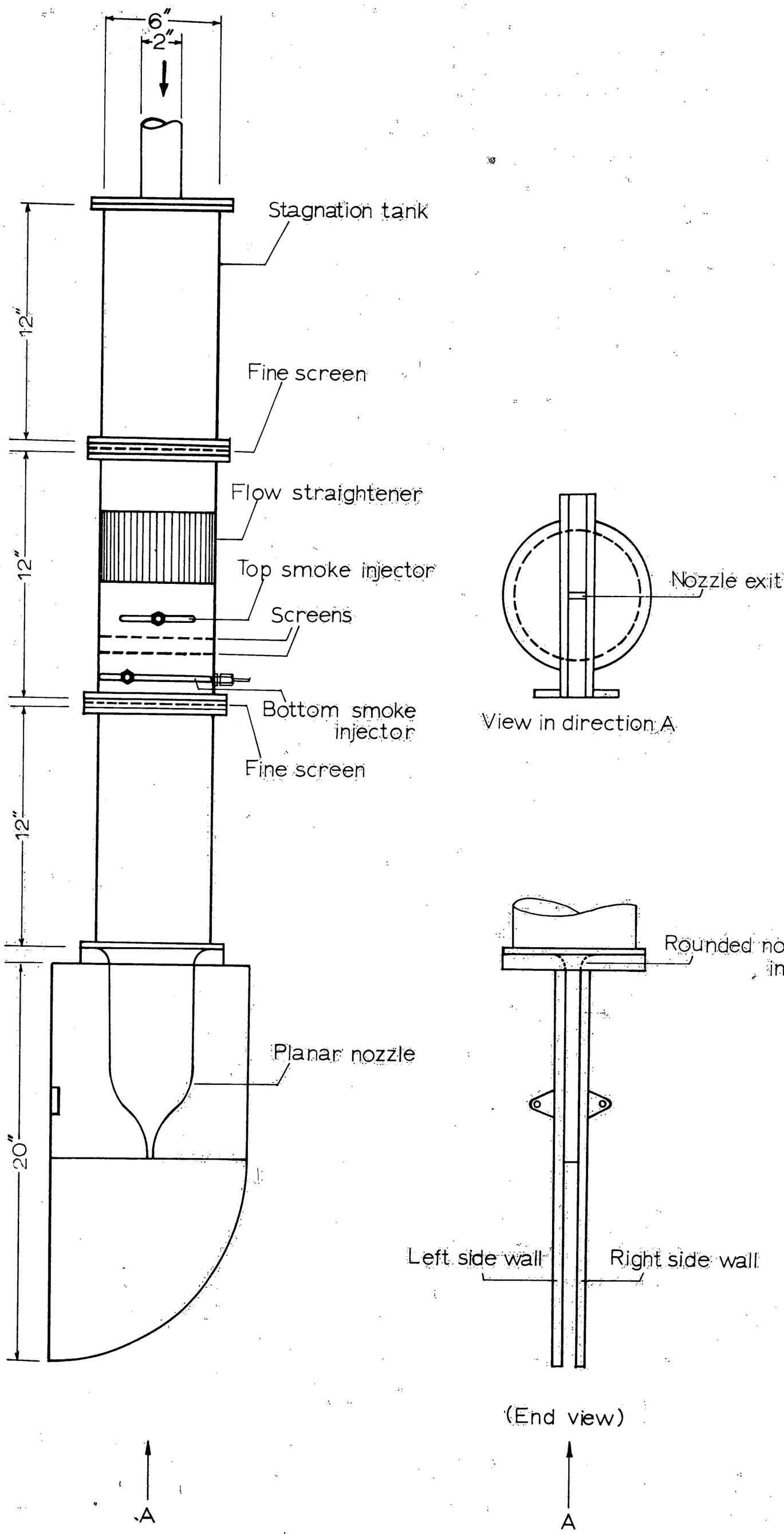
6″
2″
Stagnation tank
12″
Fine screen
Flow straightener
12″
Top smoke injector
Screens
Bottom smoke injector
Fine screen
12″
Planar nozzle
20″
A
Nozzle exit
View in direction A
Rounded nozzle inlet
Left side wall
Right side wall
(End view)
A

Figure 2

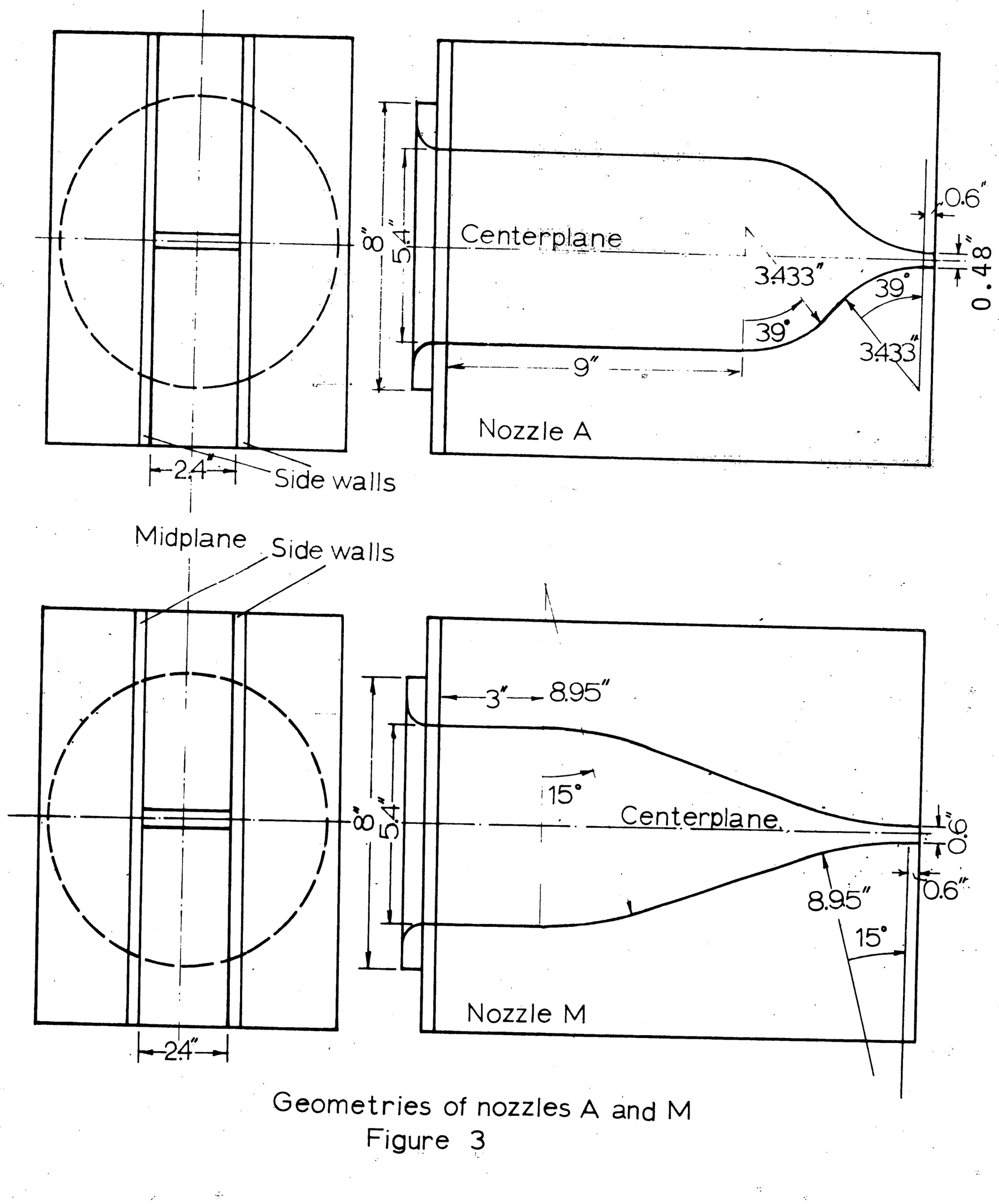

Geometries of nozzles A and M
Figure 3

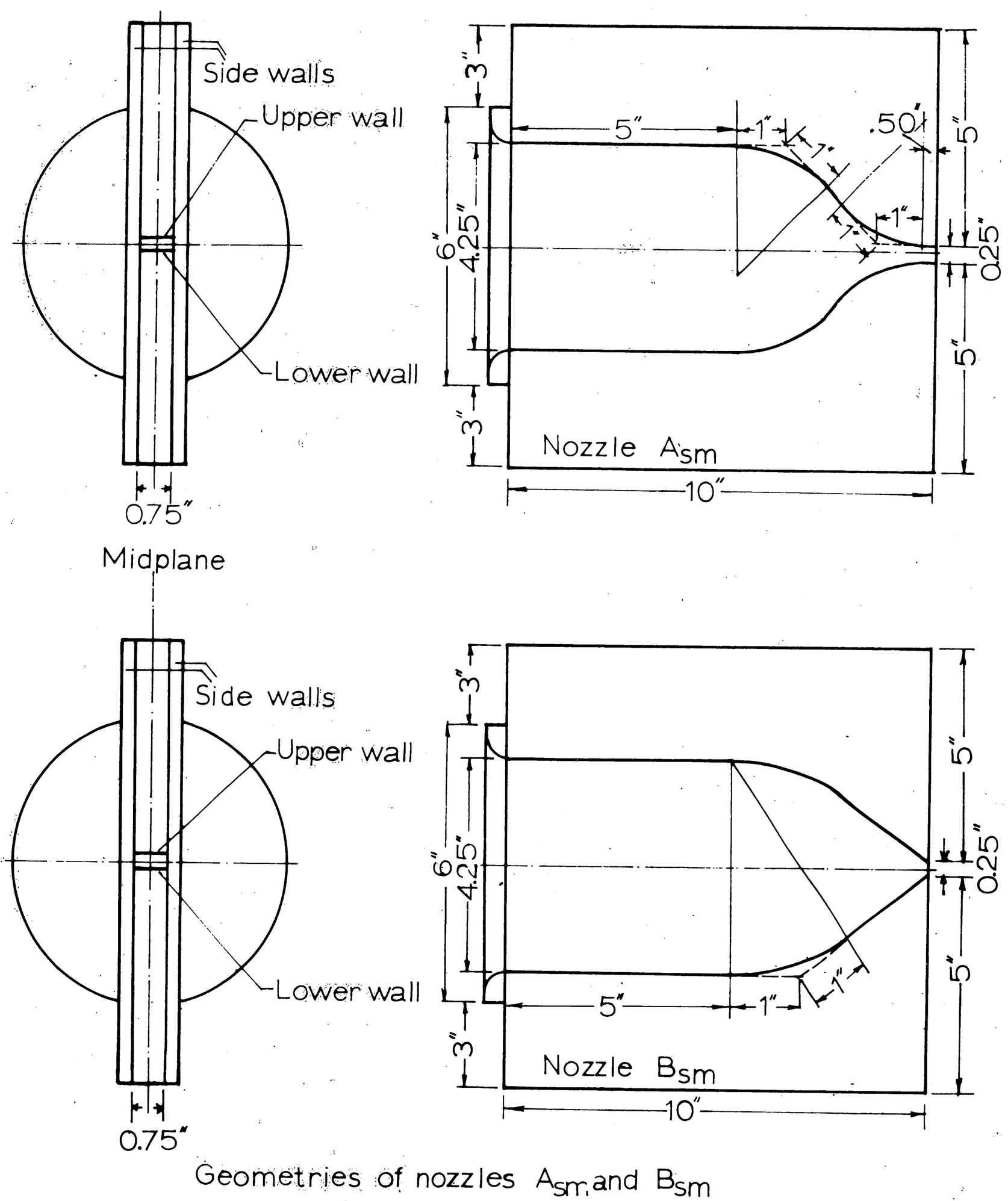

Geometries of nozzles A_{sm} and B_{sm}

Figure 4

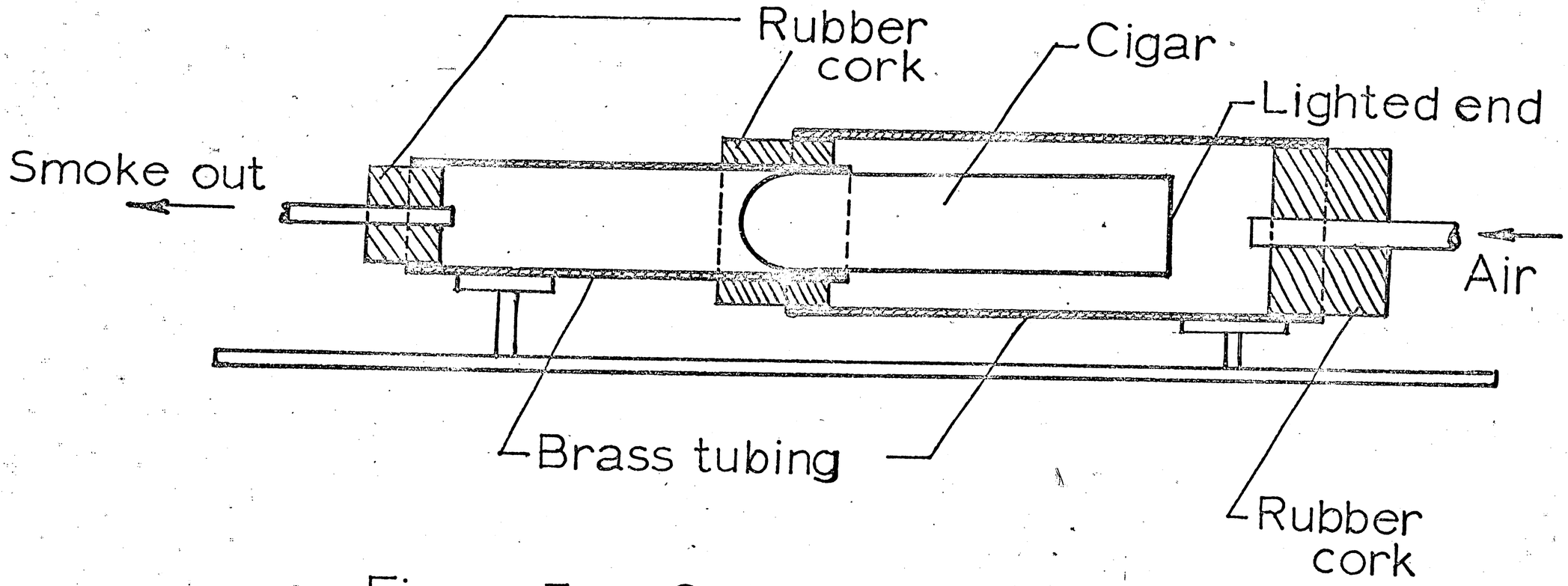

Figure 5. Smoke generator

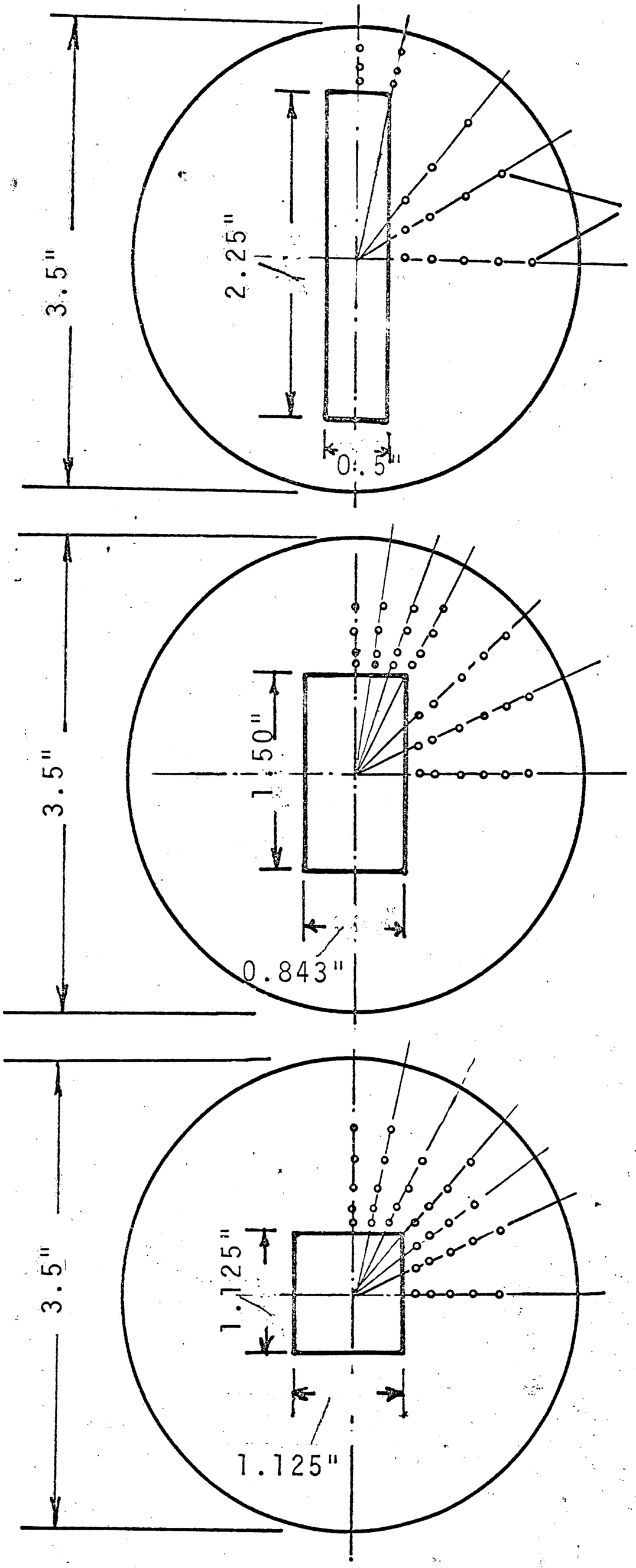

Figure 6. Nozzle inlet plates of various aspect ratios showing location of pressure taps.

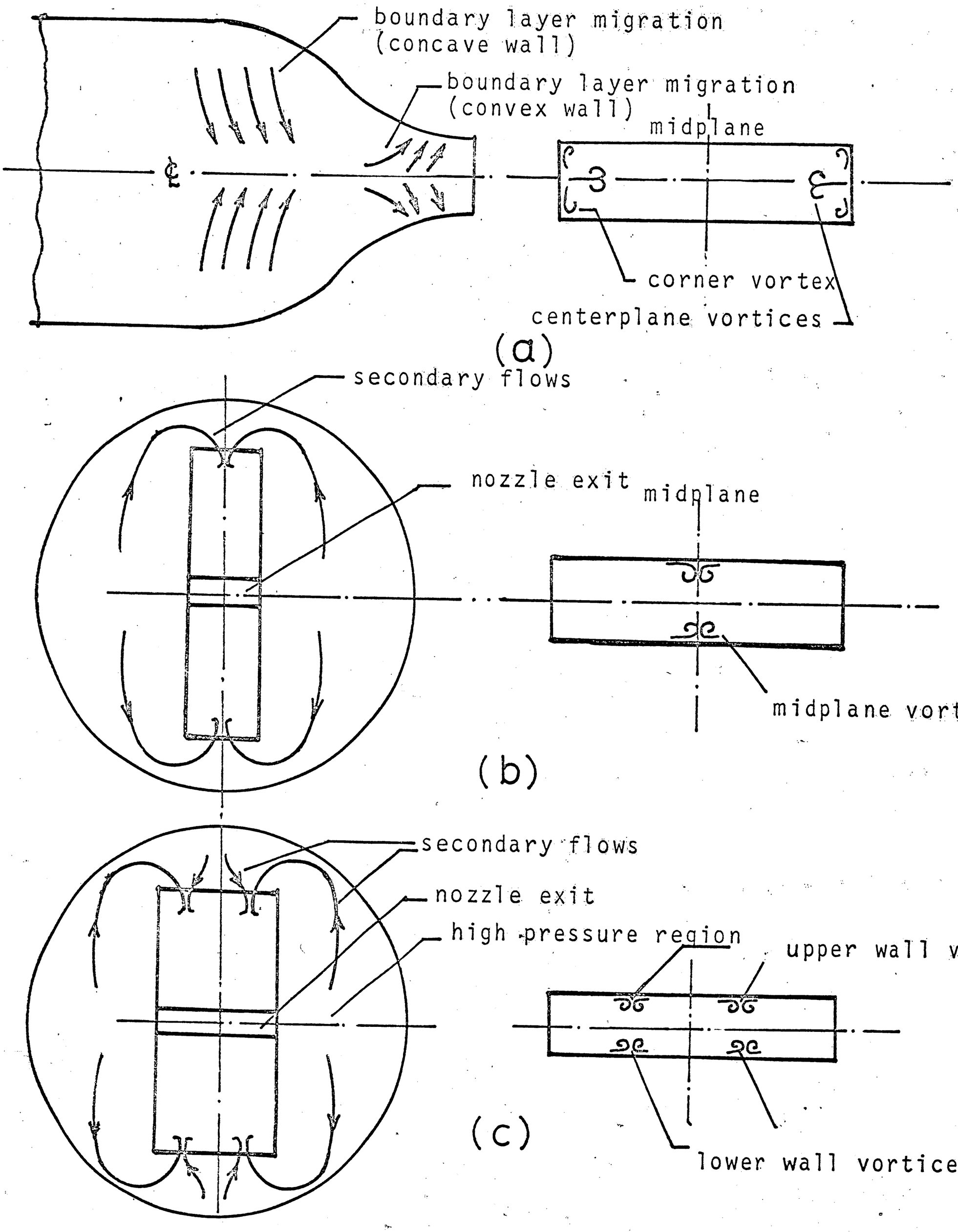

Figure 7. Origin of exit passage vortices
(a) plane wall boundary layer migration
(b) secondary flow in high inlet-aspect-ratio nozzle
(c) secondary flow in low inlet-aspect-ratio nozzle

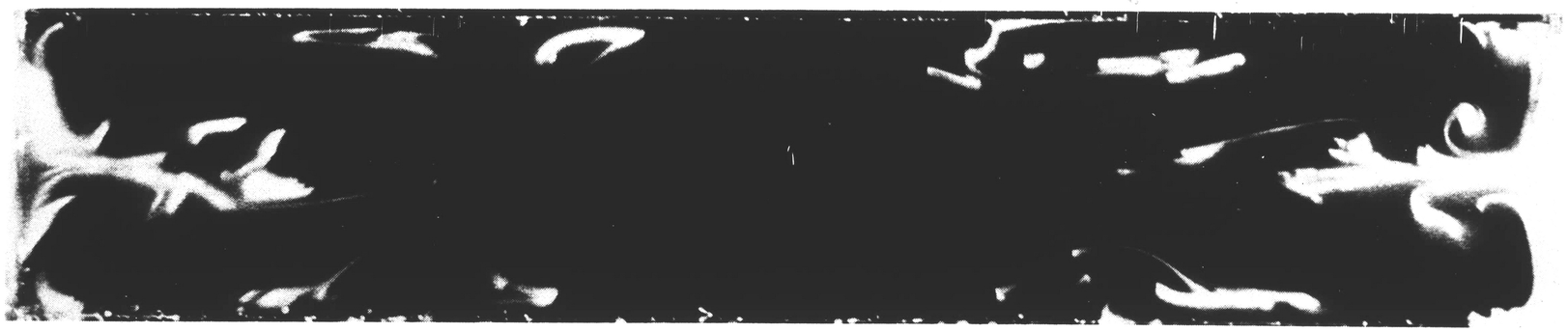

(a)

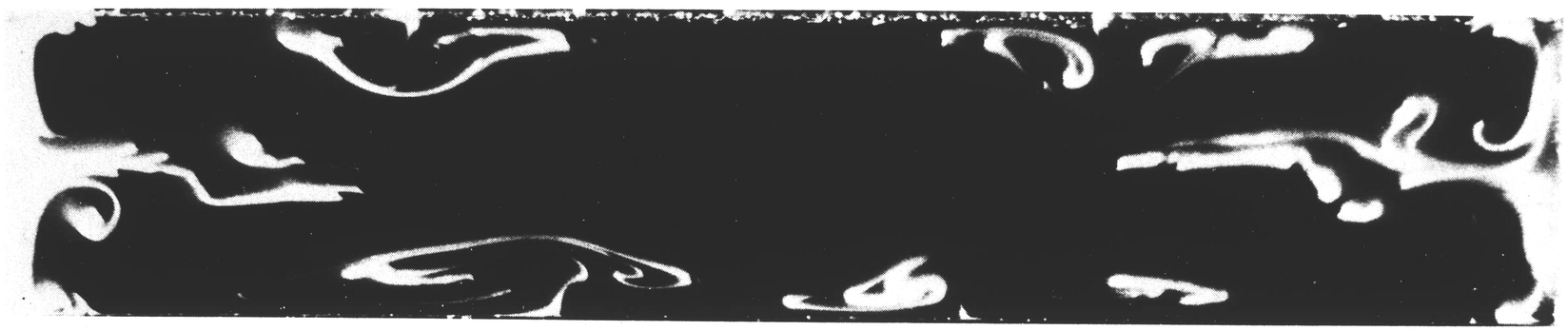

(b)

Figure 8. Nozzle A, exit aspect ratio = 5, $Re_w = 3.9 \times 10^3$.

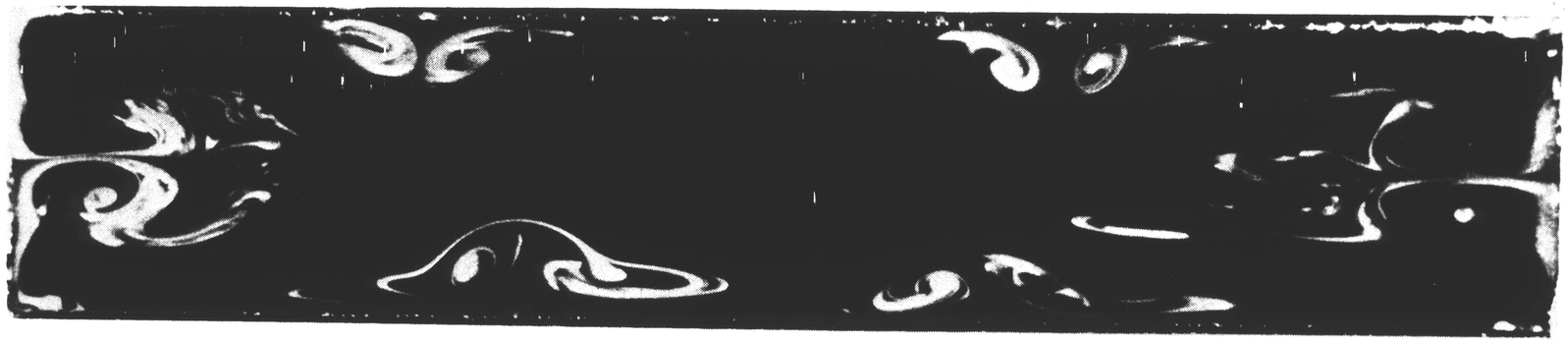

(a)

(b)

Figure 9. Nozzle A, exit aspect ratio = 5, $Re_w = 5.3 \times 10^3$.

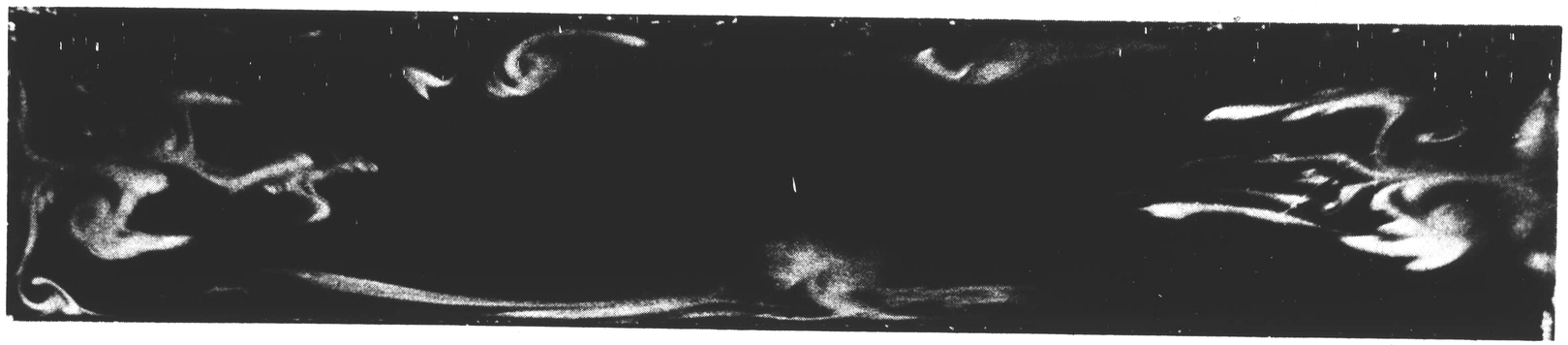

(a)

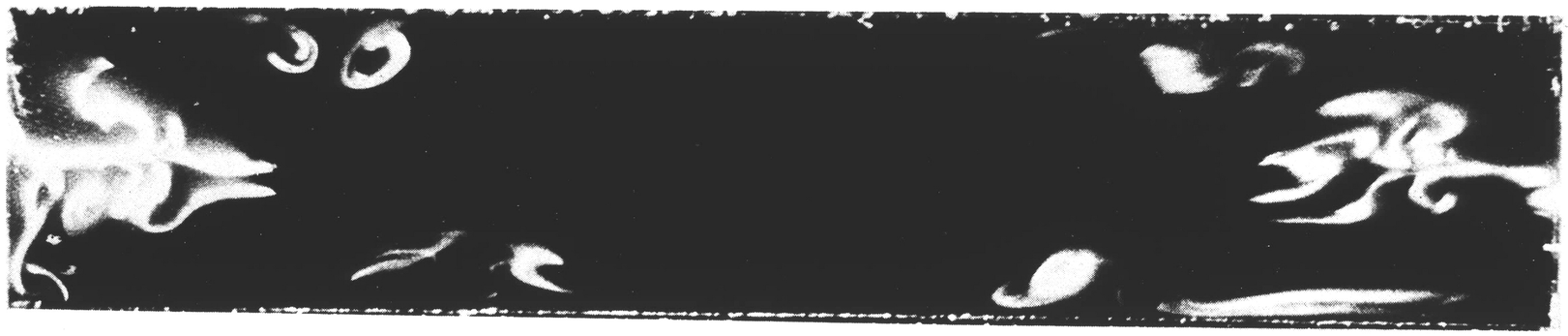

(b)

Figure 10. Nozzle A, exit aspect ratio = 5
(a) $Re_w = 6.87 \times 10^3$; (b) $Re_w = 7.4 \times 10^3$.

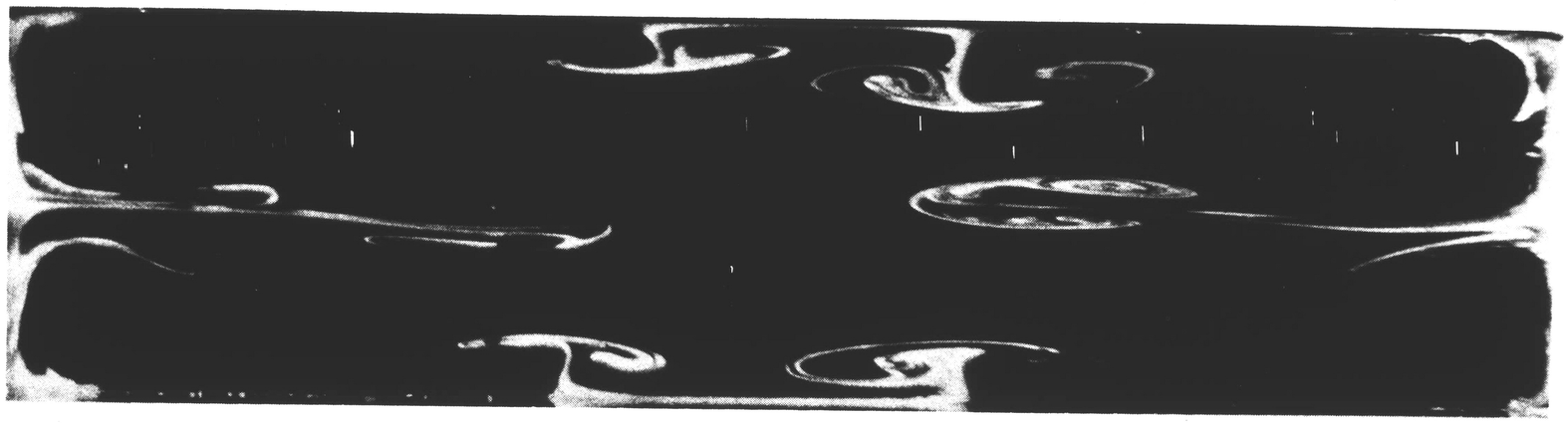

(a)

(b)

Figure 11. Nozzle M, exit aspect ratio = 4, $Re_W = 3.9 \times 10^3$.

(a)

(b)

Figure 12. Nozzle M, exit aspect ratio = 4, $Re_w = 5.3 \times 10^3$.

(a)

(b)

Figure 13. Nozzle M, exit aspect ratio = 4, $Re_W = 5.3 \times 10^3$. Distortion of vortices due to excess smoke.

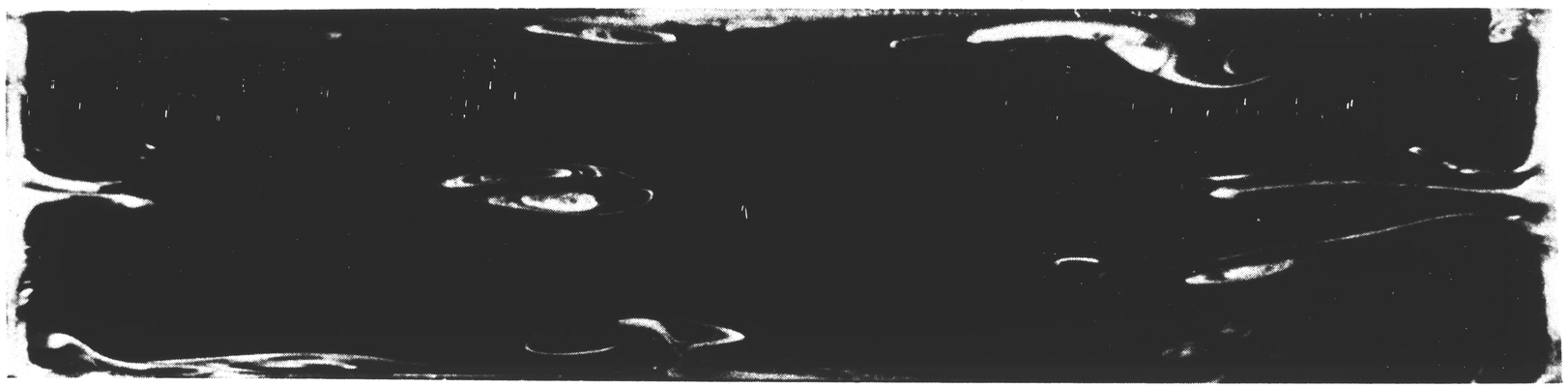

(a)

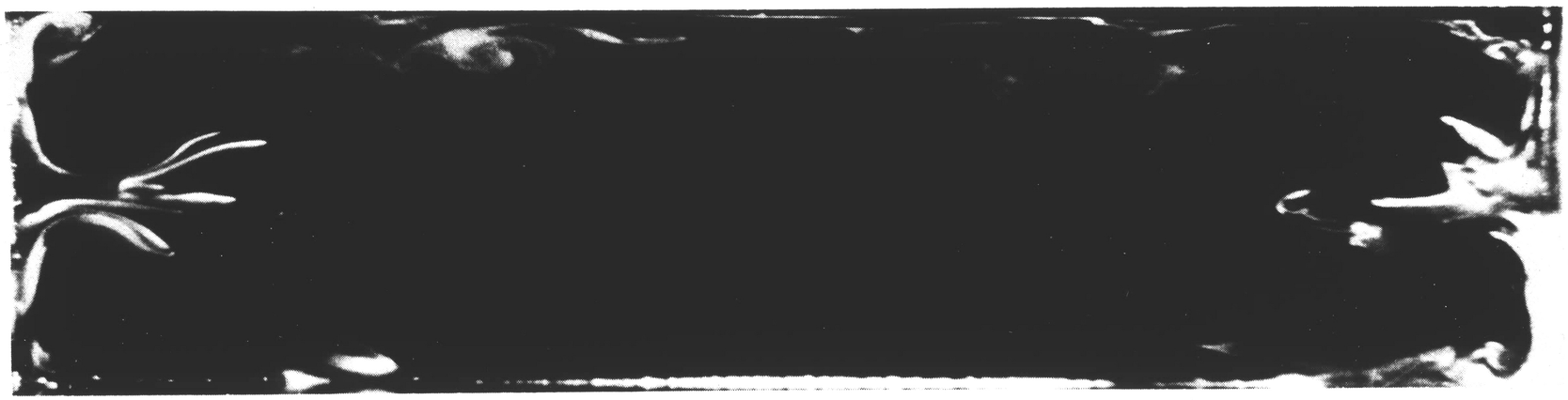

(b)

Figure 14. Nozzle M, exit aspect ratio = 4, $Re_W = 7.4 \times 10^3$.

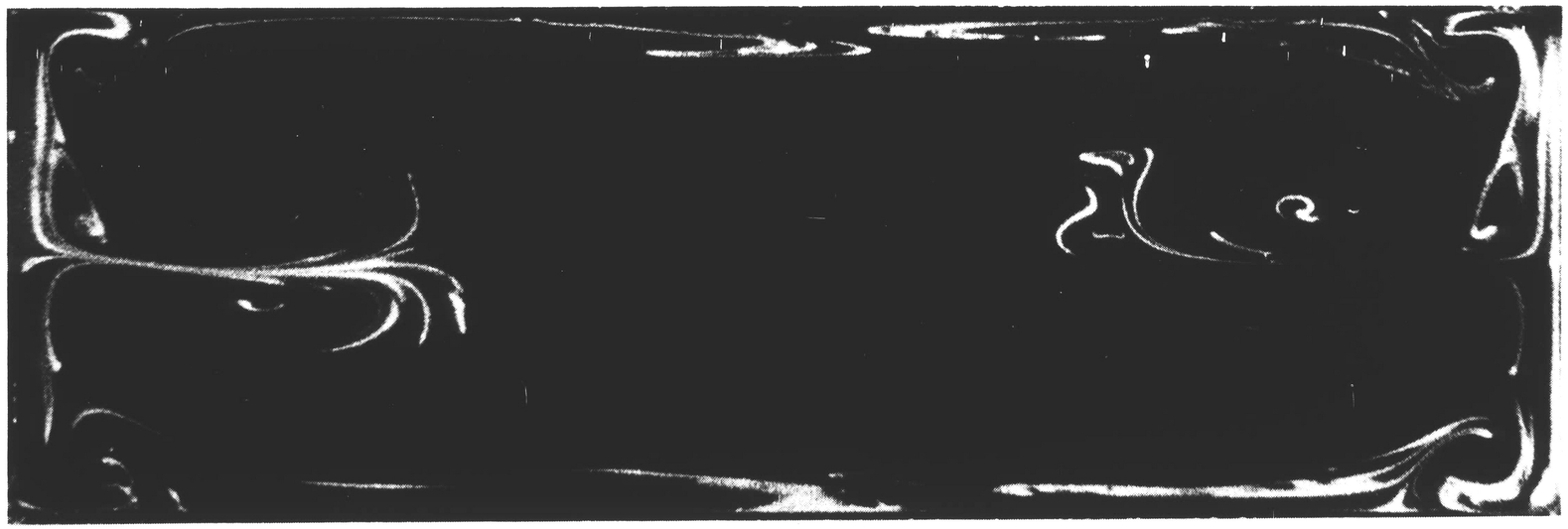

(a)

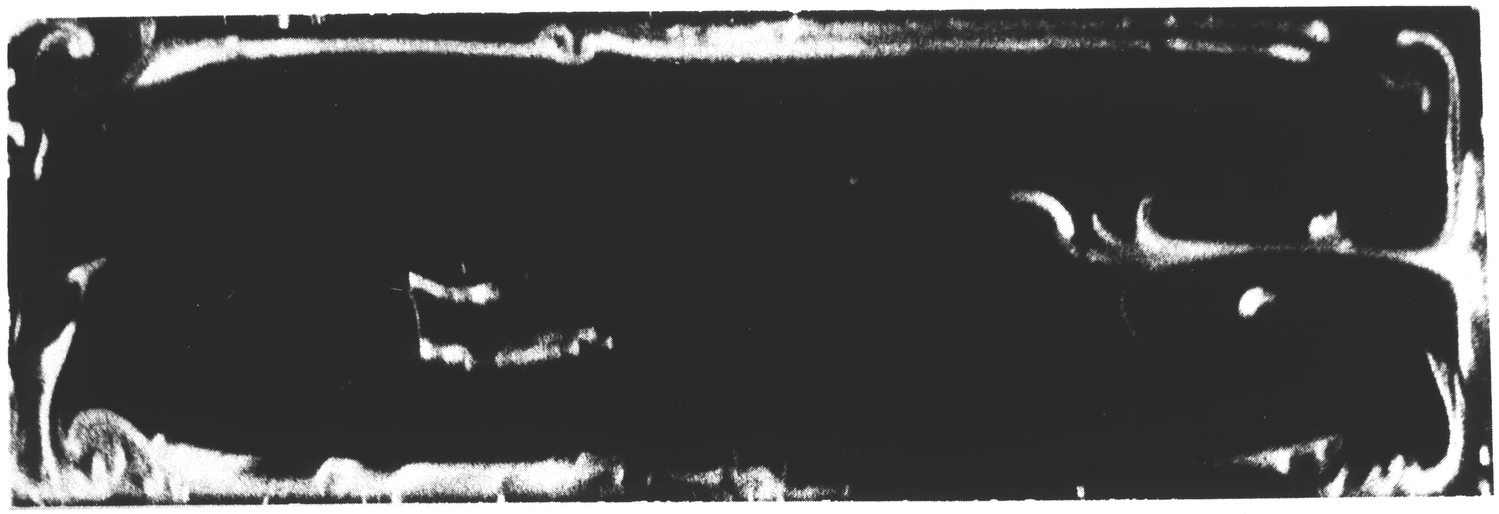

(b)

Figure 15. Nozzle A_{sm}, exit aspect ratio = 3, $Re_w = 6.7 \times 10^3$.

(a)

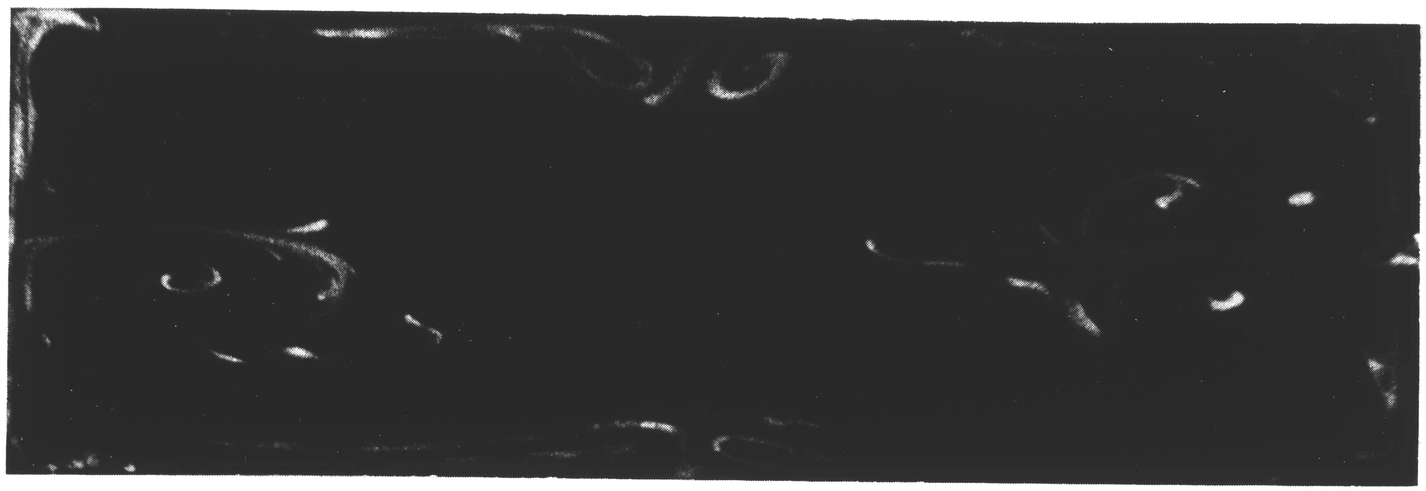

(b)

Figure 16. Nozzle A_{sm}, exit aspect ratio = 3, $Re_w = 8.5 \times 10^3$.

(a)

(b)

Figure 17. Nozzle A_{sm}, exit aspect ratio = 3, $Re_w = 1.26 \times 10^4$.

(a)

(b)

Figure 18. (a) Nozzle A_{sm}, exit aspect ratio = 3, $Re_w = 8.5 \times 10^3$. Showing flow patterns 0.5" downstream of exit passage.
(b) Nozzle B_{sm}, exit aspect ratio = 3, $Re_w = 8.5 \times 10^3$.